JOURNAL OF MATERIALS SCIENCE 33 (1998) 2683–2690

Microstructural changes on high temperature treatment of a cold-worked and nitrided Fe–1% V alloy

A. T. ÖZDEMIR, Ö. E. ATASOY
Materials Division, Metallurgy Education Department, Faculty of Technical Education, Gazi University, Ankara, Turkey
E-mail: tozdemir@tef.gazi.tr

An Fe–1.06% V alloy was used to study the control of recrystallization through fine VN precipitates in cold-worked and nitrided ferritic matrix. Nitriding was carried out at 475 °C in ammonia atmosphere. Subsequent high temperature annealing process was performed in hydrogen gas for 795, 820, 860 and 880 °C, respectively. The data on recrystallization indicates that kinetics of recrystallization obeys an Avrami type equation with a temperature independent time exponent. Transmission electron microscopy techniques were used to measure the precipitate sizes and to study the changes in the microstructure. The activation energy evaluated for recrystallization was found to be consistent with that governing the VN particle coarsening. From these findings it was concluded that the initiation of recrystallization is dominated by the interface reaction controlled growth of VN stringers at subgrain boundaries. After the disappearance of stringers, the interaction of fine precipitates with subgrain boundaries is minimized and hence recrystallization starts. © *1998 Chapman & Hall*

1. Introduction

In low alloy steels MC type carbides and MN type nitrides such as vanadium, titanium and niobium can result in effective precipitate strengthening of the steels [1, 2]. Because carbides and nitrides have very low solubility limits in ferrite than in austenite, the resulting precipitate distribution can be initially ultra fine, and therefore low alloy steels can reach high strength levels [3–5]. For high temperature application, such as for considerable creep resistance these fine precipitates have to be stable and withstand rapid particle coarsening. However, this requirement is still of prime importance for many low alloy steels even if the final usage is not intended for high temperature. Substantial particle growth may still take place during thermomechanical treatment, resulting in a consequent loss of strength. The elevated temperature stability of these fine dispersions is therefore of considerable importance. Having lower solubilities, the alloy nitrides particularly of Fe–V [6, 7] and Fe–Ti [8, 9] are known to be more stable than their respective carbides [10]. Using the detailed analysis of nitriding kinetics, in particular for Fe–1.06% V alloy [11], the present work was therefore planned to investigate the effect of heavily cold-worked substructure on the distribution of fine vanadium nitride (VN) precipitates, and so subsequent results on the high temperature behaviour of the same alloy.

2. Experimental procedure

2.1. Materials

The Fe–1.06 % V, 0.01 % C alloy used in this work was provided from BISRA in the form of 12 mm diameter hot-rolled bars. The bars were further hot-rolled to strips of 2 mm thickness, and then cold rolled to a thickness of 1 mm. Finally, rectangular specimens with the dimensions of 5×10 mm were cut from the strips and carefully cleaned for the next nitriding process.

2.2. Nitriding

Nitriding was carried out in purified ammonia (NH_3) atmosphere. Using the results of the previous work [11], and by trial and error, a nitriding temperature of 475 °C and a nitriding time of about 170 h were found to be more than sufficient for the full nitriding of the specimens without any sign of the formation of recrystallized grains. A Knoop microhardness (KHN) tester with 500 g load was used to verify the fully through thickness nitrided case. The Fe_4N phase which formed on the subscale was removed by fine grinding the nitrided specimens on each side for about 25 μm.

Nitriding was performed in a horizontal working mullite tube, within a kanthal wound furnace. The ends of the tube were tapered to fit standard glass cones, to produce gas-tight connections. While several gas purifying trains of tubes and compartments were fitted to one end, the other end was spared for housing the small specimens before the nitriding operation. The specimens were fixed to the mid-section of a silica rod via Pt hooks. One end of the rod was fitted into a soft iron sleeve, so that from outside of the sealed cone, the specimens could be controlled and moved into and out of the furnace by means of a remote magnet. During the nitriding process, the incoming

NH_3 gas first passed through a meter to control the gas flow rate and then through some soda asbestos and caustic potash containing chambers to extract the impurity CO_2, and then finally entered into the furnace. The furnace had a hot zone of about 50 mm and through Pt/Pt–13%Rh thermocouples in the vicinity of the specimen, the desired temperatures of the hot zone were maintained to within $\pm 2\,^{\circ}C$. This gas-tight system was designed to use differing gas atmospheres by switching on and off several valves to select the route for the incoming gas.

2.3. Annealing in hydrogen atmosphere

The nitrided and carefully cleaned specimens were first annealed in hydrogen (H_2) atmosphere at a medium temperature of 500 °C for about 24 h to remove the excess nitrogen from the ferrite matrix, and so to reduce the retarding effect of nitrogen on growing VN precipitates [7, 10]. After verifying by optical microscope that the microstructure was still stable, thus practically no onset of recrystallization (Fig. 1), the aforementioned specimens were then further annealed in H_2 gas for varying times at selected high temperatures of 795, 820, 860 and 880 °C to study the recrystallization behaviour. The upper temperature limit was selected as 880 °C, as ferrite to austenite phase transformation was expected at about 910 °C for the present material. The specimens were then examined to determine the fraction of recrystallization (X). Thus, thin strips of edge-wise cut specimens were mounted, polished and etched with 2% nital for metallographic examination by a Vicker's optical microscope. Lineal analysis method was used and from each specimen 20 readings were taken to determine the extent of recrystallization, and in addition, KHN measurements were taken from the same specimens to determine any effect of recrystallization upon the microhardness values.

2.4. Electron microscopy

For thin foil electron microscopy, 3 mm diameter disc specimens were thinned to about 50–60 μm thickness by gentle abrasion on wet 600 grade silicon carbide paper. Using a Struers electropolishing unit, the discs then further thinned to perforation by jet polishing, in a 5% perchloric acid, 5% acetic acid, methyl alcohol solution. At room temperature, the applied potential of 60 V, with 120 mA current was found to be a standard condition for preparing thin foils for examining in a Jeol-100 CX II electron microscope at an accelerating voltage of 100 kV. The sizes of both subgrains and vanadium nitride (VN) precipitates were measured at bright field image. Particularly, to eliminate the strain contrast effects, particle size measurements were taken from carbon replicas. Thus, the polished specimens were first etched with 2% nital for about 10–15 s and then a thin layer of carbon was evaporated on to the etched surface, after which the samples were scratched with a blade into small squares. The carbon film was next floated off by immersion in distilled water, collected on a copper grid, and finally examined by the electron microscope. The relevant measurements were made on micrographs taken from different areas of several replicas for each of the samples studied. Typically, for each temperature and several annealing times, about 500–600 particles were measured from the micrographs. Thus, the deviation from the accuracy of the measurements could not be more than $\pm 5\%$.

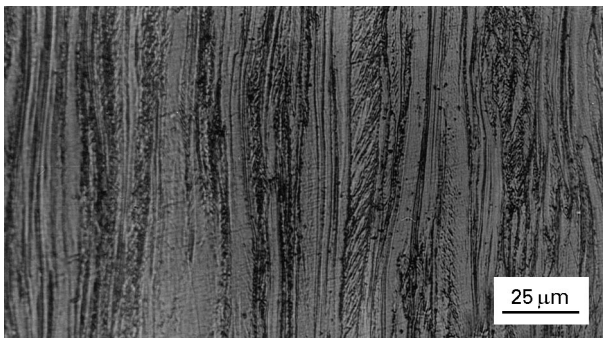

Figure 1 Typical microstructure of cold worked and nitrided Fe–1.06% V alloy.

3. Results

3.1. Microstructure

3.1.1. Recrystallization

The microstructure of partially recrystallized specimens give some indications that the recrystallized grains form by the movement of the original grain boundaries probably caused by the reduced pinning of the VN precipitates (Fig. 2). Recrystallized elongated grains seem to be built with few equiaxed grains in the centre of the specimen, while some grains at the edge of the specimen are of block shape and are large in size compared with those at the centre.

3.1.2. Hardness measurements

As shown in Fig. 3, hardness values of the nitrided and high temperature annealed specimens (at 795, 820, 860 and 880 °C) drop from the initial nitrided value of 700 KHN to a plateau of 150–160 KHN during recrystallization. A detailed analysis of hardness variation before and after the onset of recrystallization was performed on specimens annealed at 860 °C (Fig. 4). It was noticed that in 30 h hardness values reduced

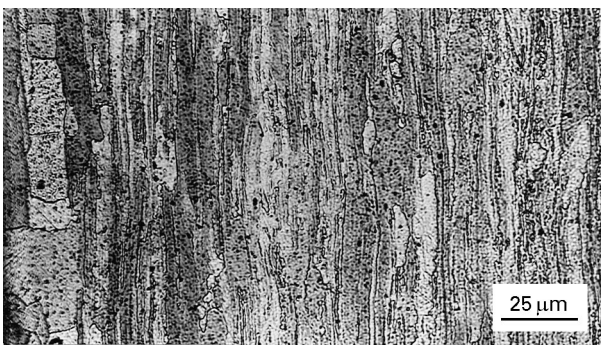

Figure 2 Micrograph showing partially recrystallized microstructure ($X \approx 0.2$) of the specimen annealed in hydrogen atmosphere at 820 °C for 500 h.

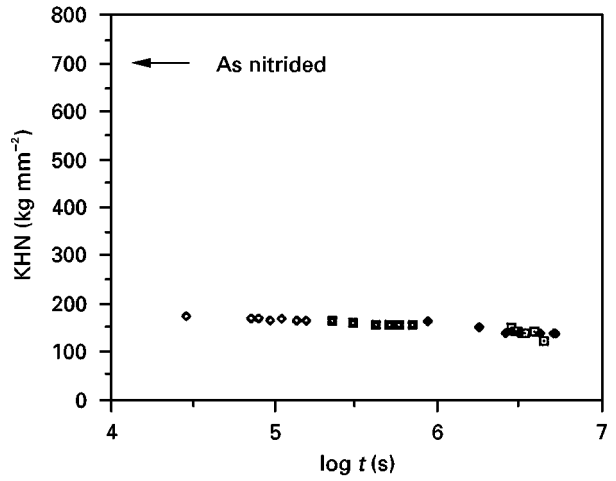

Figure 3 Change in hardness during recrystallization (⊡) 795 °C; (◆) 820 °C; (■) 860 °C; (◇) 880 °C

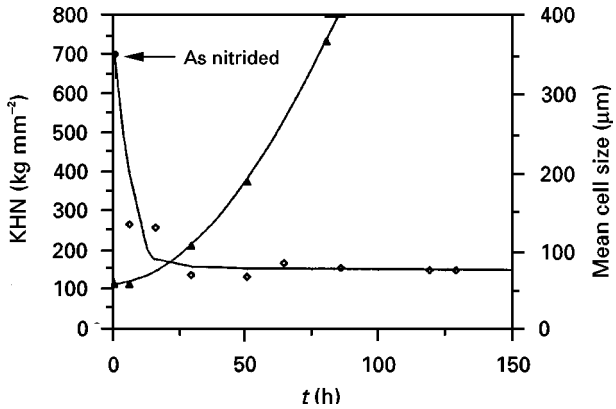

Figure 4 Changes in hardness values and subgrain sizes of the specimens annealed in hydrogen atmosphere at 860 °C; (▲) Cell size; (◇) Hardness

gradually from as-nitrided value to the plateau value. This time corresponds to about the fraction of 0.1 recrystallization, which indicates that hardness values are basically dependent on the size and the distribution of the VN precipitates, but not on the extent of recrystallization.

3.1.3. Precipitation

Nitrided microstructure consists of rectangular plate-like VN precipitates, approximately 1 nm thick (H), 4 nm length (L) and 2.5 nm width (W), where the mean aspect ratio (L/W) of the particles is about 1.6. Although in common, VN precipitate distribution seems to be homogeneous, a close up examination of transmission electron microscopy (TEM) micrographs indicates selective VN precipitation. Thus, particularly on subgrain boundaries VN precipitates form long closely spaced arrays or "stringers", in which on subsequent annealing, respective slow growth of these stringers produces a resultant bimodal VN distribution without any significant change in the aspect ratio (Fig. 11).

3.1.4. Cell size

Cell size measurements show that there is a gradual increase in cell size during recrystallization annealing from the initial cell size of about 0.6 μm for the cold worked material. As shown in Fig. 4, the beginning of the cell size increase seems to correspond to the onset of recrystallization.

3.2. Kinetics of recrystallization

The measurements of the fraction of recrystallization (X) obtained from the micrographs are plotted in Fig. 5, which shows that an Avrami type equation, $X = 1 - \exp(-kt^m)$ was obeyed with a time exponent (m) of about 1.7 irrespective to the changes in annealing temperature k is a temperature dependent factor, t is time at temperature. Thus, m values are 1.76, 1.74, 1.73 and 1.74 for 795, 820, 860 and 880 °C, respectively. From the data of recrystallization, times for the fraction of 0.5 transformation ($t_{0.5}$) were determined and from the slope of the straight line fitted to $\ln(t_{0.5})$ versus $1/T$ plot, where T is the annealing temperature in K, the activation energy for the process of recrystallization (Q_r) was calculated as 464.4 kJ mol^{-1} (111 kcal mol^{-1}) (Fig. 6).

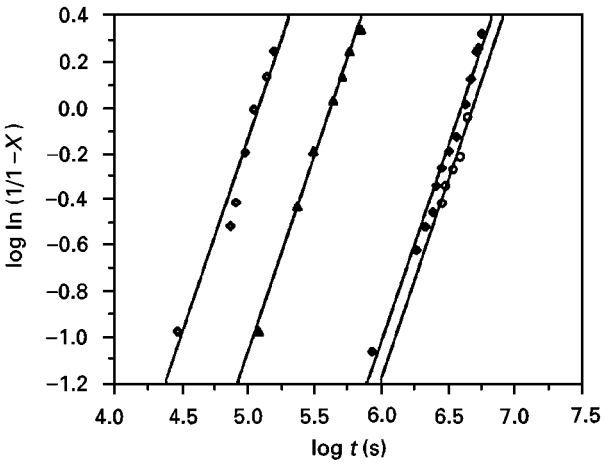

Figure 5 Dependence of recrystallization to annealing temperature. (○) 795 °C; (◆) 820 °C, (▲) 860 °C; (◇) 880 °C.

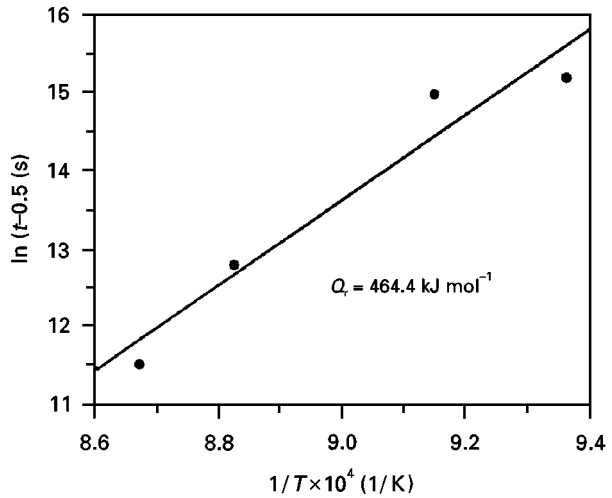

Figure 6 An Arrhenius plot for the data of recrystallization, where $t_{0.5}$ is the time for fraction of 0.5 transformation.

3.3. Kinetics of VN precipitate growth

Detailed measurements of the particle sizes were made from the micrographs taken from carbon replicas. To investigate the particle coarsening kinetics, on logarithmic scale the change in the mean particle size (L) against annealing time (t) were plotted for temperatures 820, 860 and 880 °C, respectively (Figs 7–9). For each graph, the initial nitrided precipitate size, 4 nm, was also used as the mean particle size at the beginning of annealing (but, because of being away from the area of interest, practically could not be shown in the figures). Attempts to fit a single straight line to each curve failed, then instead two different straight lines with two differing slopes were fitted. Thus at each plot, the gradient $1/n$ is initially $\approx 1/2$ for small VN sizes (shown as exp. part 1), but after reaching a transition point the slope changes to $\approx 1/3$ (shown as exp. part 2). Particularly, the second part of the curve fit is consistent with the results of a previous work [6], where extrapolated values are also shown in Figs 7–9. According to the particle coarsening theory [12, 13],

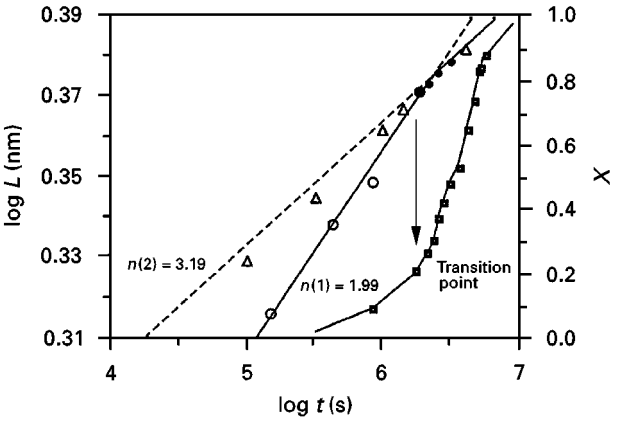

Figure 7 Time dependence of mean VN precipitate size L, and fraction of recrystallization X(■), at 820 °C, where n is the reciprocal of gradient. Exp. part 1 (○) and Exp. part 2 (●) represent the kinetics of particle coarsening before and after the onset of recrystallization respectively. Extrapolated values (△) are obtained from reference 6.

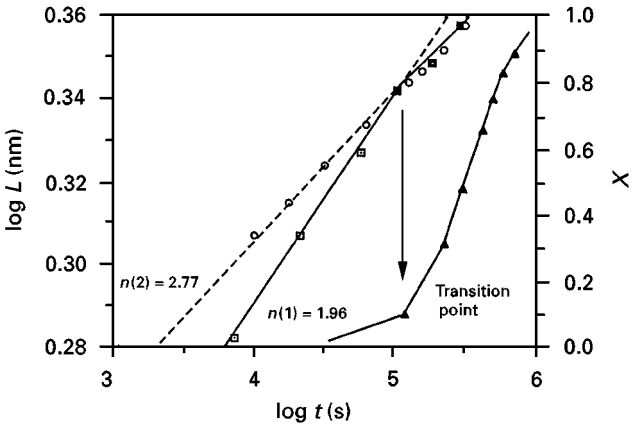

Figure 8 Time dependence of mean VN precipitate size L, and fraction of recrystallization X(▲), at 860 °C, where n is the reciprocal of gradient. Exp. part 1 (⊡) and Exp. part 2 (■) represent the kinetics of particle coarsening before and after the onset of recrystallization respectively. Extrapolated values (△) are obtained from reference 6.

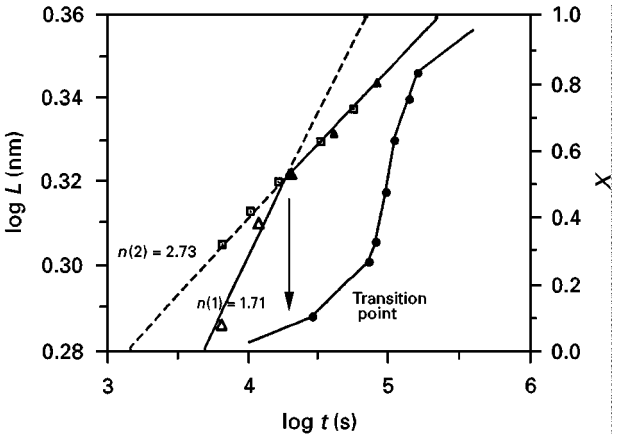

Figure 9 Time dependence of mean VN precipitate size L, and fraction of recrystallization X(●), at 880 °C, where n is the reciprocal of gradient. Exp. part 1 (△) and Exp. part 2 (▲) represent the kinetics of particle coarsening before and after the onset of recrystallization respectively. Extrapolated values (△) are obtained from reference 6.

it would be expected that $n \approx 2$ is the value for interface reaction controlled and $n \approx 3$ is for bulk diffusion controlled growth. To investigate the correlation between particle coarsening and recrystallization, on the same figure the change in fraction of recrystallization (X) with respect to annealing time was also included (Figs 7–9). It was interesting to notice that the time of changeover from $n \approx 2$ to $n \approx 3$ was always close to the time of the onset of recrystallization. An Arrhenius type analysis for the coarsening data revealed that, particularly for interface reaction controlled particle growth, the activation energy (Q_p) is about 442.7 kJ mol^{-1} (105.8 kcal mol^{-1}) (Fig. 10). This value is consistent with the value found in the work of Balliger *et al.* [10], and also in the present work very close to the activation energy found for the recrystallization (Q_r) of the cold-worked and nitrided material used.

4. Discussion

4.1. Precipitation and its morphology

It was expected that after nitriding the plate-like VN precipitates would be coherent, fine and homogeneously distributed through the ferrite matrix [8, 9, 14]. However, for the present work, TEM micrographs revealed a tendency towards heterogeneous precipitation particularly at highly populated dislocation areas, i.e. on subgrain boundaries, where precipitates were closely spaced and aligned in form of stringers. Even though it has never been observed in previous nitrided iron base alloys [6–9, 11, 14], the introduction of heterogeneous nucleation sites in the form of an array of dislocations lead to rapid precipitation; this has been confirmed in high strength aluminium alloys [15]. To eliminate precipitate free zones (PFZ), and so their deleterious effects on yield strength, it is common practice to give controlled deformation to a supersaturated aluminium alloy before ageing. For the operation to be successful, it is obvious that the rate of selective precipitation is directly

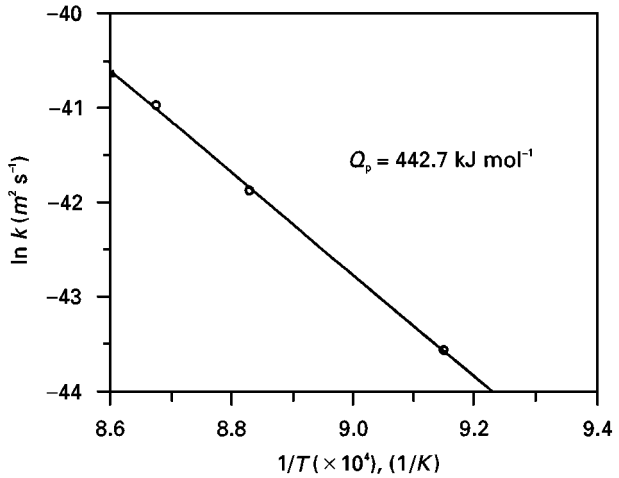

Figure 10 An Arrhenius plot constructed for the data of VN precipitate coarsening obtained from Figs 7–9, where n values are around 2.

proportional to the density of dislocation substructure. The rate of precipitation has to exceed the rate of recovery of the cold-worked substructure. It was stated that, if the alloy recrystallized before the start of precipitation, the deformation stage then had no useful value [15, 16].

During nitriding of the present material, the formation of the VN precipitates may be due to reducing the overall lattice strains. It was previously stated that dissolved nitrogen atoms have the tendency to move towards the strain fields of the lattice defects, especially around dislocations [9]. Thus, similar to the development of Cottrell atmospheres as solute segregation at dislocation cores [17], in the present heavily deformed material, a selective settlement of dissolved nitrogen on cold worked substructure, i.e. subgrain boundaries, may likely have the same intention, such as to optimize the overstraining of the lattice. Consequently, high concentration of nitrogen atoms may attract vanadium atoms and so a selective precipitation of fine VN particles (stringers) on subgrain boundaries may be enhanced.

4.2. Subgrain growth

It was Zener [18] who first considered the fundamentals of particle interactions with moving boundaries. However, Zener model was a rough approach, as he only considered random distribution of particles and rigid grain boundaries. The problem was first treated for a curved boundary by Hellman and Hillert [19], and further improved for the assumption that a boundary will bow forward between randomly dispersed particles [20, 21]. Conversely Duggan and Hutchinson [22] suggested a different model for a low angle boundary, in which almost all of the particles lie on the subgrain boundaries. According to their findings, the impinging force created by fine particles on subboundaries are relatively higher than that on high angle boundaries. In a recent work where subgrain growth was investigated experimentally, it was found that at 70% cold-rolled material (A1–4Cu), particles of θ (Al_2Cu) could be seen mostly on subboundaries [23]. On subsequent annealing at about 280 °C, under the control of precipitates, subgrains grew respectively slower than the theoretically predicted rates, where subgrain growth satisfied the parabolic growth law. Hence, it was concluded that, theoretical models particularly derived for subgrain growth controlled by particles situated on the subgrain boundaries were not suitable to make accurate predictions. Hence for the present work, it is obvious that stringer formation along subgrain boundaries may be strongly active in retarding the subgrain growth.

4.3. Mode of recrystallization

Study of the recrystallization kinetics in the present work shows that the time exponent (m) of the Avrami type equation is around 1.7. According to Cahn [24], this value indicates site saturation for nucleation, where recrystallization is restricted to original grain boundaries. Examination of the recrystallized microstructure at low magnification confirms the original boundary migration during recrystallization, and may suggest that VN precipitate retardation is severe, and so all subgrain boundaries are immobilized together with original grain boundaries till the onset of recrystallization. This may be partially supported through the work of Gladmann [25], who suggested that VN precipitates in ferrite retarded both recovery and recrystallization, but rather initiation of recrystallization was from strain-free subgrains after reaching a certain critical size [25, 26]. Hansen *et al.* [27] and Crooks *et al.* [28] who investigated the effect of VCN, NbCN precipitates on dynamic and static recrystallization of austenitic matrix is microalloyed steels were also in agreement with the initiation of recrystallization from subgrains. However, they both stressed on an effective size of fine precipitates, suggesting that, in the absence of particle coarsening there was no sign of recrystallization.

The basic nucleation mechanism in recrystallization may still not seem to be definite. Therefore, the present results may discriminate such viable mechanisms as subgrain growth [29, 30], and strain induced boundary migration [31, 32]. As shown in Fig. 4, in the present work the initial cold worked cell size is about 0.6 μm. This value is 1/3 of the value given for pure iron deformed by 10% [33]. Thus, as the degree of cold work for the present material is about 50%, the present work suggests that, an increase in the extent of deformation results in a gradual decrease in the cell size. TEM micrographs indicate that at high magnification, i.e. substructural scale, during high temperature annealing subgrains at first grow slowly, and then fast after the onset of recrystallization, which suggests that recovery is taking place under the control of slowly growing VN precipitates, i.e. continuous recrystallization [16]. However, at low magnification scale nucleation of recrystallization may seem to be in the form of original boundary migration (discontinuous recrystallization), [16]. For example, the start up of recrystallization seems to be highly non-uniform, and many of original boundaries remain inactivated

as nucleation sites. The actual case on the other hand may be in the form of particle controlled continuous slow growth of subgrains, where the recrystallized microfronts migrate into the unrecrystallized areas. As cleaning up the traces of cold work, i.e. dislocations, at the near original boundary regions, subgrains may induce the original boundary to move to form visible bulges. Thereafter, grain boundaries may migrate faster than subboundaries, because it has been stated that during recrystallization retardation of fine precipitates is large on subboundaries than on original boundaries [27, 34].

4.4. Particle coarsening and its effect on recrystallization

Previous observations indicated at least some degree of substructural enhancement of diffusion. Through a first work in a quenched and tempered steel, where many subboundaries in the matrix were expected from the decomposition of martensite, it was found that for particle coarsening at intermediate temperatures (500 °C), the time exponent $1/n$ was approximately 1/5 (dislocation pipe diffusion) [35]. However, as the temperature increased (700 °C), the initial value of $1/n$ for dislocation pipe diffusion rose through 1/4 (boundary diffusion) to 1/3 (volume diffusion). Further studies demonstrated that if the quenched and tempered structure of subboundaries linking all the particles were to be eliminated by recrystallization, the particle coarsening rate was much reduced [36, 37]. Moreover, a creep deformation applied before coarsening which reintroduced a dislocation substructure raised the coarsening rate again by about three orders of magnitude [38]. A similar result was also reported for an aluminium–copper alloy having subboundaries through cold work, after the precipitation of fine θ (Al_2Cu) particles [39]. In recent works, in microalloyed steels that contained VCN precipitates in austenite, the effect of 5% cold work on particle coarsening was dislocation pipe diffusion, reported as the control mechanism, where in the microstructure there was no sign of significant subgrain formation due to cold work [10]. In case of severely cold-worked microalloyed steels where fine TiC and NbCN particles precipitated before the deformation, it was concluded that formation of migrating recrystallization front and thus the start of recrystallization is caused by the particle coarsening which was found to be volume diffusion controlled [40]. Other workers however, investigated more complex phenomena as effect of continuous and discontinuous VCN, NbCN precipitation on dynamic and static recrystallization during and after hot rolling of austenitic matrix [27, 28, 41]. Rather than homogeneous, a selective fine heterogeneous precipitation on grain boundaries and cold-worked substructure, in particular prior to recrystallization, was found to be very effective in retarding and stopping the recrystallization of the material. Even a bimodal particle size distribution was noticed caused by preferential coarsening of precipitates on either subboundaries or dislocations [27]. Some recent workers in particular concentrated on the growth kinetics of strain induced fine precipitates that settled on dislocations and subboundaries, experimentally [41] and analytically [42]. In their findings, it was stated that rather than a single mechanism, two differing mechanisms of solute transfer took place simultaneously to coarsen the precipitates, such as pipe diffusion and volume diffusion, where on the average particle size was noticed to increase (by time)$^{1/3}$ law, caused by large surface area of particle available to volume diffusion. So consequently, prior plastic deformation was suggested to play an important role in the geometry as well as the kinetics of subsequent precipitation and particle growth. However, in none of these studies were attempts made to evaluate the time exponent $1/n$, as different from 1/3, and no work has further been published which attempted to check if the details of the subboundary enhanced diffusion theories are correct. The general conclusion is, hence, that the theories described seem successful in accounting qualitatively for the effect of lattice defects on particle coarsening.

In the present work, hardness results indicate considerable softening of the matrix at early stages of annealing (Fig. 4). Regarding the retarded onset of recrystallization, softening seems to be not because of recrystallization but is from VN precipitate growth. For the current alloy, the VN coarsening kinetics in the absence of subgrains was previously studied [6, 7]. It was reported that in H_2 atmosphere, the time exponent was 1/3 and therefore was consistent with the volume diffusion controlled law [11, 12]. The activation energy for the process was found as 211.7 kJ mol^{-1} (50.6 kcal mol^{-1}), and was close to the energy of activation for vanadium diffusion in ferrite matrix [6]. A similar investigation was also studied elsewhere in nitrided microalloyed austenitic vanadium steels, in which again growth of VN precipitates was controlled by volume diffusion and the energy of activation was within the limits of vanadium diffusion in austenite, i.e. 357.7 kJ mol^{-1} (85.5 kcal mol^{-1}) [43]. However, in the present work, according to the findings, interface-controlled and volume-diffusion-controlled coarsening mechanisms seem to be in competition (see Figs 7–9). At the beginning of annealing, the precipitates within subgrains start to grow by (time)$^{1/3}$ law, whereas the precipitates along subgrain boundaries, i.e. stringers, start to grow later by (time)$^{1/2}$ law. While both mechanisms are active, particularly before the onset of recrystallization, stringers density is relatively high and therefore is effectively controlling the whole precipitate coarsening process. With respect to extrapolated volume diffusion results (Figs 7–9), retardation of coarsening rate for interface controlled growth may be caused by very close spacing of fine VN precipitates along the stringers.

There are some observations from several previous works that may be explanatory for the present situation. For the present work, it has been found that in some cases surface reaction controlled coarsening may govern the overall rate of particle growth. Particularly, before the onset of recrystallization, it seems that the slowest step in the coarsening process is the transfer of atoms across the precipitate/matrix

interface. At the beginning of high temperature annealing, the matrix is full of stringers, and therefore very close spacing of VN precipitates is inevitable. This in return obviously may reduce the growth of precipitates in common. Thus, being encounters at very closely spaced precipitates, dissolution paths between particles may overlap, and so the precipitate matrix interface may be saturated with excess solute atoms. It was verified through a previous work that the dissolution kinetics of precipitates were slowed down because of concentrated solute atoms around particles, and so reduced magnitude of the concentration gradient [44, 45]. The initial surface reaction controlled growth may also be explained by the presence of slowly migrating ultra fine coherent VN precipitates. In general at plate-like precipitates, having coherent character, precipitate/matrix interfaces rotate to achieve low energy orientations. It was suggested that [46], by virtue of their good crystallographic fit, plate-like precipitates would be expected to be immobile. Thus usually, coherent interfaces were less mobile than incoherent ones so that there would be retarded rates of migration of precipitate/matrix interfaces. There are only a few cases so far reported that the growth kinetics obey $(\text{time})^{1/2}$ law [47, 48], where the available explanation for the change in kinetics was made through the presence of immobile interfaces. But rather as verified in some previous works [7, 10] this may be coupled with the selective contamination of VN interfaces by excess nitrogen atoms and thus in return with the reduction in the misfit of the precipitate/matrix interface (reducing the interfacial energy). Contamination of the precipitate/matrix interface with impurities was also verified elsewhere. Thus, the presence of impurities such as oxygen had marked influence on the growth of Si_3N_4 [49] and Fe_4N [50] precipitates in ferrite and in both cases the growth mechanism changed from volume diffusion control to interfacial control when a critical oxygen potential was exceeded. Consequently, based on these observations, for the present work, it is possible to state that the growth kinetics of VN precipitates may be affected adversely and rather than volume diffusion, interface diffusion may be expected within highly populated fine VN precipitate arrays. It is because of this selective slow growth of particles within the stringers, with respect to the fast growing (volume-diffusion-controlled) precipitates inside the subgrains, a bimodal precipitate distribution is inevitable and was observed in micrographs (Fig. 11). Around the time for onset of recrystallization, the density of stringers decreases, and coarse VN precipitates inside the subgrains may take the lead, the overall particle growth mechanism then transfers from interface-controlled to diffusion-controlled with time exponent of 1/3; thereafter, recrystallization initiates and proceeds gradually. Thus, slow particle growth at subboundaries, i.e. stringers, controls the growth of subgrains and so depresses the incubation time for recrystallization. This is confirmed by the close values of calculated activation energies for recrystallization and particle coarsening kinetics (see Figs 6 and 10). From Figs 7–9 (consider the related transition points), it is clear that as annealing temperature increases, the onset of recrystallization takes place at a smaller mean precipitate size. This observation is reasonable, because both rates of nucleation and growth of new strain free grains and so the mobilities of high angle boundaries surrounding these grains are temperature dependent [16, 34]. Thus, as annealing temperature increases, the rate of grain boundary migration also increases. To immobilize the boundaries of these new formed recrystallized grains and so to retard the onset of recrystallization, a smaller mean VN precipitate size or interparticle spacing is therefore necessary [34, 39].

Figure 11 TEM micrograph showing bimodal distribution of VN precipitates at 860 °C annealed for 6 h.

5. Conclusions

The results of the present work show that;

1. Through nitriding of the cold worked Fe–1.06%V alloy, plate-like VN fine precipitates are almost uniformly distributed in the matrix, but long arrays of precipitates (stringers) along subgrain boundaries also seem to have a considerable fraction in the total distribution of the precipitates.
2. During annealing of the material, on the average a changeover from $(\text{time})^{1/2}$ law to $(\text{time})^{1/3}$ law in particle coarsening occurs. Thus, a transition from interface reaction controlled coarsening to diffusion controlled coarsening takes place. This has been attributed to the reduction in the initially highly populated density of the stringers, which finally is responsible for the bimodal VN precipitate distribution.
3. The aforementioned changeover in the kinetics of particle growth is in coincidence with the initiation of recrystallization, suggesting that the onset of the recrystallization is retarded and controlled by the slow growth of VN precipitates on subgrain boundaries.
4. Activation energies have been calculated for both the kinetics of recrystallization and that of particle coarsening, and the results are also evident that controlling mechanism in the onset of recrystallization is the interface reaction controlled growth of VN precipitates.

Acknowledgements

The authors would like to thank the Metallurgical Engineering Department of the Middle East Technical

University, Ankara, Turkey, for providing the use of laboratories and research installations.

References

1. T. GLADMANN, I. D. MCIVOR and D. DULIEU, in Proceedings of the International Conference on Microalloying 75, Washington, USA October 1975. p. 32.
2. R. W. K. HONEYCOMBE, *Met. Trans. A* **7A** (1976) 915.
3. B. ARONSSON, in "Climax molydenum symposium on steel str. mechanisms" (Zürich, Switzerland, 1969) p. 77.
4. H. SEKINE, *Trans. Iron Steel Inst. Jpn.* **8** (1968) 101.
5. R. W. FOUNTAIN and J. CHAPMAN, *Trans. Met. Soc. AIME* **212** (1958) 737.
6. S. BOR and Ö. E. ATASOY, *Tubitak Doga Dergisi* **4** (1980) 1.
7. Ö. E. ATASOY, *Met. Trans. A* **14A** (1983) 379.
8. *Idem*., *Trans. JIM* **17** (1976) 625.
9. H. D. KIRKWOOD, Ö. E. ATASOY and S. E. KEOWN, *Met. Sci.* **8** (1974) 49.
10. N. K. BALLIGER and R. W. K. HONEYCOMBE, *ibid.* **4** (1980) 121.
11. S. BOR and Ö. E. ATASOY, *Met. Trans. A* **8A** (1977) 975.
12. M. LIFSHITZ and V. V. SLYOZOV, *J. Phys. Chem.* **19** (1961) 35.
13. C. WAGNER, *Z. Metallkd.* **61** (1970) 108.
14. M. POPE, P. GRIEVESON and K. H. JACK, *Scand. J. Met.* **2** (1973) 29.
15. J. W. MARTIN, in "Micromechanisms in partical hardened alloys" (Cambridge University Press, London, 1980) p. 39.
16. U. KÖSTER, *Met. Sci.* **8** (1974) 151.
17. A. H. COTTRELL and B. A. BILBY, *Proc. Phys. Soc.* **A62** (1951) 490.
18. C. ZENER, *J. Appl. Phys.* **20** (1949) 950.
19. P. HELLMAN and M. HILLERT, *J. Scand. Metall.* **4** (1975) 211.
20. P. M. HAZZLEDINE, P. B. HIRSH and N. LOUAT, in "Recrystallization and Grain Growth in Multi Phase and Partical Containing Materials", edited by, N. Hansen, A. R. Jones and T. Leffers (Risø, National Lab., Roskilde, Denmark, 1980) p. 85.
21. E. NES, N. RYUM and O. HUNDERI, *Acta Metall.* **33** (1985) 11.
22. B. J. DUGGAN and W. B. HUTCHINSON, in Proceedings of the 4th European Conference on Texture and the Properties of Materials, The Metals Society, London, UK, 1975) p. 292.
23. S. K. CHANG, *Met. Sci. Technol.* **8** (1992) 760.
24. R. W. CAHN, *Acta. Metall.* **4** (1956) 449.
25. T. GLADMANN, I. D. MCIVOR and F. B. PICKERING, *J. Iron Steel Inst.* **209** (1971) 380.
26. T. GLADMANN, in "Recrystallization and Grain Growth in Multi Phase and Partical Containing Materials", edited by, N. Hansen, A. R. Jones and T. Leffers (Risø, National Lab., Roskilde, Denmark, 1980) p. 183.
27. S. S. HANSEN, J. B. WANDERSANDE and M. COHEN, *Met. Trans. A* **11A** (1980) 387.
28. M. J. CROOKS, A. J. GARRATT-REED, J. B. VANDER SANDE and W. S. OWEN, *Met. Trans. A* **12A** (1981) 1999.
29. H. HU, in "Electron Microscopy and Strength of Crystals" (Interscience, New York, 1963) p. 546.
30. J. C. M. LI, *J. Appl. Phys.* **33** (1962) 2958.
31. P. A. BECK and P. R. SPERRY, *ibid.* **21** (1950) 150.
32. J. E. BAILEY, *Phil. Mag.* **5** (1960) 833.
33. A. S. KEH and S. WEISSMANN in "Electron Microscopy and Strength of Crystals", edited by, G. Thomas and J. Washburn (Interscience, New York, 1963) p. 231.
34. R. D. DOHERTY, *Met. Sci.* **8** (1974) 132.
35. O. BANNYH, H. MODIN and S. MODIN, *Jernkontorets Ann.* **146** (1962) 774.
36. W. E. STUMPF and C. M. SELLARS, in "The Mechanism of Phase Transformations in Crystalline Solids" (Institute of Metals, London, 1969) p. 120.
37. T. MUKHERJEE and C. M. SELLARS, in "The Mechanism of Phase Transformations in Crystalline Solids" (Institute of Metals, London, 1969) p. 122.
38. R. D. DOHERTY and J. W. MARTIN, *Trans. Amer. Soc. Met.* **57** (1964) 874.
39. F. J. ASHBY, in "Recrystallization and Grain Growth in Multi Phase and Partical Containing Materials", edited by, N. Hansen, A. R. Jones and T. Leffers (Risø, National Lab., Roskilde, Denmark, 1980) p. 324.
40. U. LOTTER, W. MÜSCHENBORN and E. THIEMANN, in "Recrystallization and Grain Growth in Multi Phase and Partical Containing Materials", edited by, N. Hansen, A. R. Jones and T. Leffers (Risø, National Lab., Roskilde, Denmark, 1980) p. 133.
41. B. DUTTA, E. WALDES and C. M. SELLARS, *Acta Metall.* **40** (1992) 653.
42. J. J. HOYT, *ibid.* **39** (1991) 2091.
43. P. FERGUSON, J. H. DRIVER and A. HENDRY, *J. Mater. Sci.* **18** (1983) 2951.
44. D. L. BATY, R. A. TANZILLI and R. W. HECKEL, *Met. Trans.* **1** (1970) 1651.
45. H. B. AARON and G. R. KOTLER, *ibid.* **2** (1971) 393.
46. H. I. AARONSON, C. LAIRD and K. R. KINSMAN, in "Phase transformations" (American Society for Metals, ASM, Metals Park, Ohio, Chapman & Hall, London, 1970) p. 313.
47. D. M. SCHWARTZ and B. RALPH, *Phil. Mag.* **19** (1969) 1069.
48. A. YOULE, D. M. SCHWARTZ and B. RALPH, *J. Met. Sci.* **5** (1971) 131.
49. W. ROBERTS, P. GRIEVESON and K. H. JACK, in Proceedings of the International Symposium on Metallurgical Chemistry (Iron and Steel Institute, Sheffield and London, 1971) p. 384.
50. P. HAYES and P. GRIEVESON, *Met. Sci.* **9** (1975) 332.

Received 11 November 1996
and accepted 5 February 1998